CSIRO PUBLISHING

RESEARCH FRONT

Aust. J. Chem. **2014**, *67*, 1309–1317
http://dx.doi.org/10.1071/CH14217

Full Paper

Nonstabilised Azomethine Ylids from *N*-Oxides: Unravelling the Deprotonation of *N*-Methylmorpholine *N*-Oxide

Paul Malek Mirzayans,[A] *Elizabeth H. Krenske,*[A] *and Craig M. Williams*[A,B]

[A]School of Chemistry and Molecular Biosciences, University of Queensland, Brisbane, Qld 4072, Australia.
[B]Corresponding author. Email: c.williams3@uq.edu.au

Nonstabilised azomethine ylids (NAYs) are useful 1,3-dipoles, but their synthetic applications are restricted by the high temperatures often needed for their generation, and by an incomplete understanding of the effect of heteroatoms in cyclic systems. We have examined the behaviour of *N*-methylmorpholine *N*-oxide (NMO) as a NAY precursor in the Roussi reaction (low-temperature reaction of an *N*-oxide with strong base). The choice of base is critical to achieving cycloadduct formation. We report synthetic and computational (density functional theory) investigations of the products obtained with different bases and their mechanisms of formation.

Manuscript received: 4 April 2014.
Manuscript accepted: 7 May 2014.
Published online: 4 June 2014.

Introduction

Azomethine ylids **1**, both nonstabilised azomethine ylids (NAYs) and stabilised azomethine ylids (SAYs), are versatile reactive intermediates that undergo (3+2) cycloadditions onto double and triple bonds to afford pyrrolidines **2** and dihydropyrroles **3**, respectively (Scheme 1).[1] These reactions have found widespread application in organic synthesis and have been used in the total synthesis of complex natural products[1,2] and in materials chemistry.[3]

Many of the leading procedures to generate NAYs require high temperatures. A few methods can be conducted at room temperature, but only a handful are compatible with the use of low temperature (e.g. −78 to 0°C).[1] Methods that allow the use of low temperature involve 2-azaallyl anions (metallated 1,3-dipoles),[1b,4] desilylation of iminium salts,[1c,5] ring opening of aminals,[6] and double deprotonation of tertiary amine *N*-oxides (Roussi reaction[7]). Of these four classes, only the latter three are amenable to the preparation of N–R (as opposed to N–H) substituted cycloadducts.

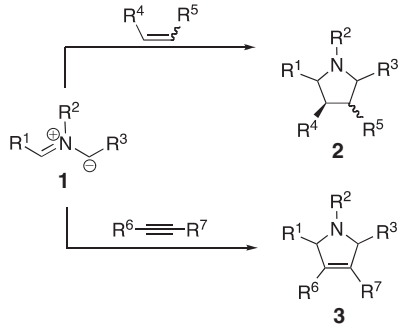

Scheme 1. Azomethine ylid (3+2) cycloadditions.

In the Roussi reaction (Scheme 2),[8] a tertiary amine *N*-oxide[9] is treated with a strong base (typically lithium *N*,*N*-diisopropylamide, LDA) in the presence of a dipolarophile to afford the (3+2) cycloadduct(s). In terms of *N*-oxide functionality, Roussi's method has mostly been applied to *N*-oxides bearing simple alkyl substituents (e.g. Scheme 2a, b). Intramolecular cycloadditions[10] (but not intermolecular cycloadditions[11]) have been accomplished with *N*-benzyl systems, while there are several examples of intermolecular cycloadditions involving *N*-allyl[12] and *N*-phenyl[11] derivatives. With respect to heteroatom-containing substituents, β-hydroxy *N*-oxides (Scheme 2c) undergo reaction, but also lead to significant amounts of side products, including cyclic aminals[13,14]; these reactions are often dominated by azomethine dimerisation,[14] which is also commonly observed in other applications of Roussi's method. *t*-Butyl ethers are tolerated,[13] and have been used in an attempt to promote chiral induction,[15] but the subsequent removal of the *t*-butyl group requires use of the aggressive reagent trimethylsilyl iodide.[16]

During investigations directed towards the synthesis of morpholine type-containing natural products, we sought to perform a (3+2) cycloaddition using the NAY generated from *N*-methylmorpholine *N*-oxide (NMO, **4**). While the corresponding non-oxygenated heterocycle, *N*-methylpiperidine *N*-oxide (NPO, **5**) has been used as a NAY precursor by Roussi (e.g. Scheme 2b),[1,17] a survey of the literature revealed that reactions involving morpholine-derived *N*-oxides lacked precedent.

We discovered that NMO (**4**) is a challenging substrate for Roussi-type chemistry. The incorporation of the oxygen atom into

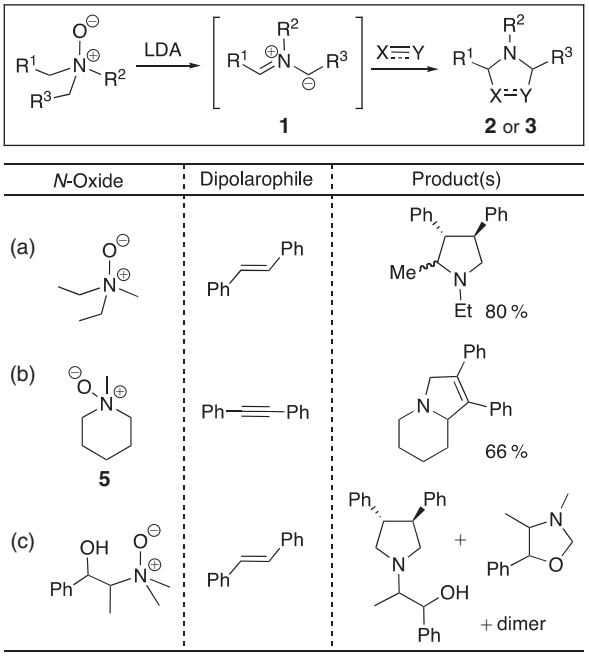

Scheme 2. Roussi's method for generation and (3+2) cycloaddition of NAYs.

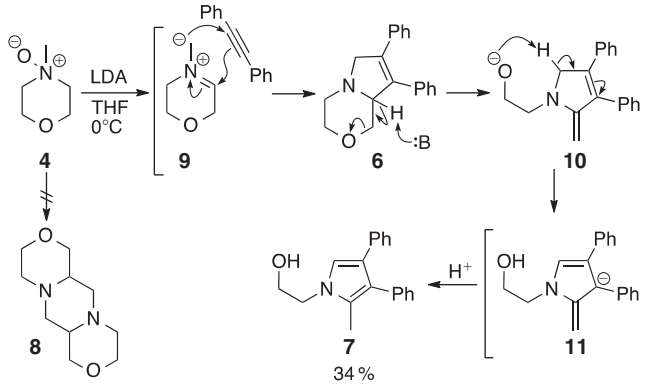

Scheme 3. Reaction of NMO (**4**) with LDA and diphenyl acetylene leading to pyrrole **7**.

the six-membered ring leads to a complex array of side reactions, which are sensitive to the nature of the base. We have used a combination of experimental and computational methods to examine the products obtained under different conditions and their mechanisms of formation. We herein report our studies of the reactions of NMO (**4**) with strong bases and reveal the factors that must be addressed in developing a protocol for azomethine ylid generation from this class of heteroatom-containing *N*-oxides.

Results and Discussion

Our initial studies focussed on the behaviour of NMO (**4**) under the conditions typically used by Roussi (LDA, THF) (Scheme 3). In contrast to NPO (**5**) (Scheme 2b), treatment of a suspension of NMO (**4**) with 3.5 equiv. of LDA in the presence of diphenyl acetylene (THF, 0°C) did not lead to isolation of the expected cycloadduct **6**. Instead, pyrrole **7** was obtained in 34 % yield (Table 1, entry 1). Although the yield of **7** was modest, no azomethine ylid dimer **8** was isolated as a side product. Increasing the concentration of base by three-fold

Table 1. Reaction condition screening in the synthesis of azomethine ylids arising from NMO

Entry	Addition rate	Base	Equiv.	Temp.	Yield.	Product
1	10 min	LDA	3.5	0°C	34 %	**7**
2	15 min	LDA	10	0°C	27 %	**7**
3	1 h	LDA	3.5	0°C	10 %	**7**
4	45 min	*n*-BuLi	3.5	0°C	8 %	**7**
5	15 min	MDA	3.5	0°C	18 %	**6**
6	10 min	MDA	3	−50°C → r.t.	17 %	**6**
7	15 min	MDA	6	0°C	18 %	**6**

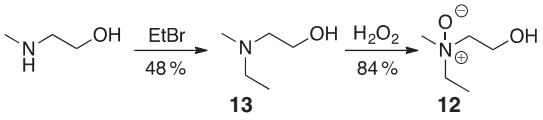

Scheme 4. Synthesis of *N*-oxide **12**, a possible decomposition product of NMO.

slightly decreased the yield of **7** to 27 % (Table 1, entry 2). Conceptually, the formation of **7** could commence with azomethine ylid formation (i.e. **9**) and (3+2) cycloaddition giving **6**. Then, a sequence involving deprotonation of **6**, C–O bond cleavage giving **10**, and proton transfer from C to O may furnish **11**, which gives **7** upon protonation (Scheme 3).

In an attempt to minimise the possibility of rearrangement of **6** to **7**, we performed a modified protocol in which the concentration of LDA was kept low by addition via syringe pump to the suspension of NMO (**4**) and diphenyl acetylene (THF, 0°C) over a period of 1 h (Table 1, entry 3). This protocol, however, decreased the yield to 10 %. Again, no dimer **8** was isolated. Using *n*-butyl lithium (*n*-BuLi) instead of LDA, and conducting the addition over a period of 45 min did not improve upon these results (Table 1, entry 4). At higher rates of addition, *n*-BuLi added to the triple bond of diphenyl acetylene (a similar result was also observed for *t*-butyl lithium, *t*-BuLi). During the slow addition of LDA described above, a transient intermediate was detected by TLC. It is possible that this intermediate was cycloadduct **6**, however, another possibility is that one of the C–O bonds of NMO (**4**) cleaves before an azomethine ylid is generated, and it is the ring-opened ylid that undergoes cycloaddition. To probe the latter possibility, we subjected the acyclic *N*-oxide **12** (prepared as in Scheme 4) to the same conditions. The *N*-oxide **12** is a plausible ring-opened decomposition product of NMO. It was synthesised from *N*-methylethanolamine and ethyl bromide via intermediate **13**. When *N*-oxide **12** was treated with LDA at −78°C, only a trace amount of pyrrole **7** was formed. This suggests that *N*-oxide decomposition is not the primary origin of pyrrole **7** during the reaction of NMO (**4**) with LDA.

We studied the behaviour of NMO under increasingly basic conditions. Treatment of a suspension of NMO (**4**) with *t*-BuLi in THF at −72°C, followed by slow warming to −30°C over 4 h, afforded a complex mixture. Surprisingly, the aqueous phase contained some unreacted NMO (**4**), together with minor impurities. Similar results were observed when the reaction was quenched at −72°C rather than being allowed to warm to −30°C. Unfortunately, reliable quantification of the various species in the aqueous phase was not possible, due to the presence of inorganic salts. Further increasing the base strength by employing Schlosser's base (*t*-BuLi/*t*-BuOK)[18] at −72°C

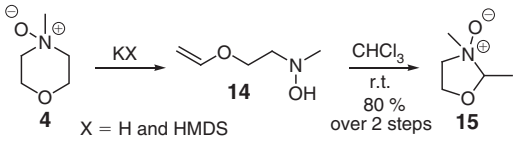

Scheme 5. Reaction of NMO (**4**) with potassium bases leading to **14** and subsequently **15**.

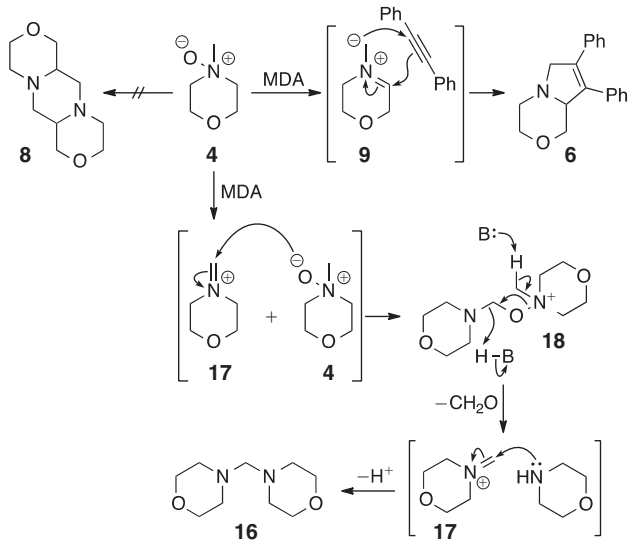

Scheme 6. Reaction of NMO (**4**) with MDA and diphenyl acetylene leading to cycloadduct **6** and side product **16**.

afforded a complex mixture of compounds that suggested decomposition rather than azomethine ylid formation.

Because the deprotonation of NMO (**4**) involves metal-coordinated species, we turned our attention to the effect of varying the metal cation. When potassium hexamethyldisilylazide (KHMDS) was added to a suspension of NMO (**4**) and diphenyl acetylene (THF, 0°C), the reaction cleanly afforded the hydroxylamine **14**, which was stable enough to be isolated (Scheme 5). In chloroform, **14** converted to **15** via a reverse Cope elimination[19] on standing overnight (80 % yield over two steps, **4** to **15**). Use of potassium hydride (KH) required elevated temperature (60°C), but likewise afforded **14** (33 %). The non-oxygenated heterocycle NPO **5** does not react under these conditions.

Treatment of NMO (**4**) and diphenyl acetylene with the sodium base NaHMDS gave no product. The NMR spectrum of the crude mixture revealed unreacted NMO (**4**) and diphenyl acetylene. The same outcome was obtained when sodium *N*,*N*-diisopropylamide (NDA)[20] was used as the base.

After the lack of success in generating the desired cycloadduct **6** by using Li^+, Na^+, or K^+ bases, we investigated a magnesium base. Pleasingly, treating a mixture of NMO (**4**) and diphenyl acetylene (THF, 0°C) with commercial magnesium bis(*N*,*N*-diisopropylamide)[21] (MDA) gave the expected cycloadduct **6** in 18 % yield (Scheme 6) (Table 1, entry 5). With **6** at hand, we were able to obtain pyrrole **7** in 71 % yield (82 % based on recovered starting material, brsm) by simply treating **6** with LDA at 0°C. This result supports the intermediacy of **6** in the synthesis of **7** under these conditions. Heartened by these results, we systematically examined variations in reaction conditions in an attempt to obtain a more favourable yield of **6**. Conducting the reaction at −50°C and slowly warming to room temperature (r.t.) gave a slightly lower yield (Table 1, entry 6), while increasing the quantity of MDA from 3 to 6 equiv. gave no change in yield (Table 1, entry 7).

Additives such as 1,3-dimethyl-3,4,5,6-tetrahydro-2(1*H*)-pyrimidinone (DMPU) and tetramethylethylenediamine (TMEDA)[22] were benign, whereas magnesium bromide etherate complex substantially retarded product formation. Different combinations in rates of addition, and order of addition of reagents, gave no improvement in the yield. No reaction was observed when MeMgBr was substituted for MDA. Finally, when the reaction was conducted in the absence of diphenyl acetylene, no dimer **8** was detected, but the Polonowski-type[23] adduct **16**[24] was isolated (~70 %). A possible mechanistic route to **16** (Scheme 6) involves mono-deprotonation of NMO and elimination of $^-OMg(NH^iPr_2)(N^iPr_2)$ to give the iminium cation **17**, which is attacked by a second molecule of NMO (**4**) to give **18**. In the presence of excess base, **18** decomposes with expulsion of formaldehyde to give iminium ion **17** and morpholine, which combine to form **16**. Interestingly, the production of a gas was observed during the experiment, which is presumably formaldehyde.[25b] The decomposition of NMO (**4**) via the pathway **4** → **17** → **18** → **17** is an autocatalytic process that has previously been proposed by Rosenau and co-workers, who also observed gas production due to formation of formaldehyde.[25] Having observed **16** as a substantial by-product under the aforementioned conditions we believe that the low yield of **6** observed in the reaction of NMO (**4**) and diphenyl acetylene with MDA is due to the formation of **16**. (Note: Rosenau and Kosma have proposed that the conversion of **18** to **17**, plus formaldehyde and morpholine, may be either intermolecular (as drawn), or alternatively, intramolecular via a 6-membered transition state (TS) where deprotonation is effected by the nitrogen lone pair.[25])

As obtention of different products upon treatment of NMO (**4**) and alkyne with Li^+, K^+, and Mg^{2+} bases was highly unexpected we performed density functional theory (DFT) calculations to explore the mechanistic origins of these products. The reactions of NMO (**4**) with diphenyl acetylene and base in THF were computed at the SMD/B3LYP-D3/6–31G(d) level of theory, modelling the base as $MNMe_2$ ($M^+ = Li^+$, K^+, or $Mg(NMe_2)^+$). This simple approach to modelling bases containing different metal cations does not make any allowance for the effects of aggregation or solvent coordination, and therefore will not give quantitative accuracy in the prediction of absolute rates. Nevertheless, it is expected to give useful qualitative insights into the way in which the identity of the metal cation influences the barrier for a given process, and thus the observed chemoselectivity.

The initial calculations (Fig. 1) examined the relative reactivities of NMO (**4**) and NPO (**5**) towards azomethine ylid formation under Roussi's conditions (LDA in THF). Roussi proposed[12] that the reaction of **5** with LDA commences with deprotonation of the *N*-Me group (*exo* deprotonation, **TS1**), which is kinetically more facile than deprotonation of one of the methylene groups adjacent to nitrogen (*endo* deprotonation). *Exo* deprotonation and loss of $^-OLi(NHR_2)$ lead to iminium cation **19**, which is deprotonated again to give azomethine ylid **20**. Calculations employing $LiNMe_2$ as the base (Fig. 1, dashed line) indicate that the rate-limiting step of this pathway is the cleavage of the N–O bond of the intermediate lithiated carbanion **21** (**TS2**). In agreement with Roussi's proposal, *exo* deprotonation of NPO (**5**) is kinetically more favourable than *endo* deprotonation. The *endo* TS is 1.5 kcal mol^{-1} higher in energy

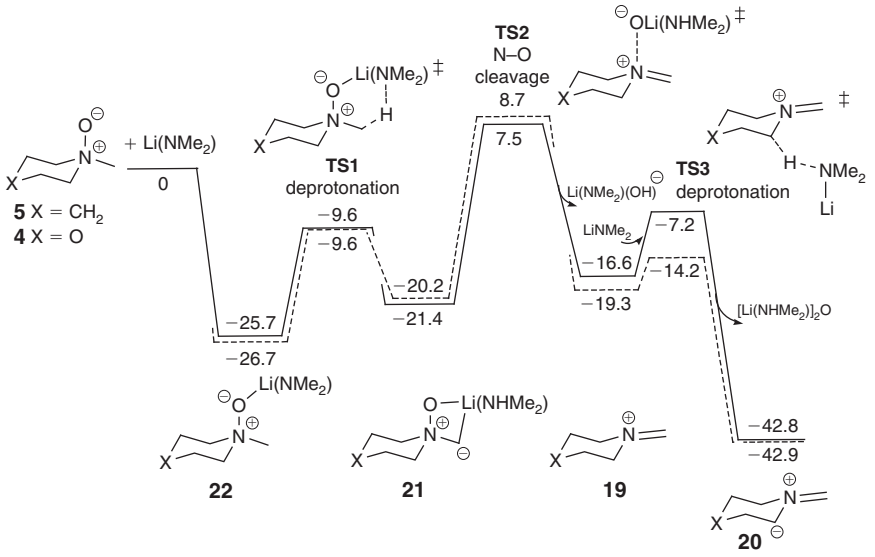

Fig. 1. Free energy diagrams for $LiNMe_2$-mediated azomethine ylid formation from NMO (**4**) and NPO (**5**) in THF, computed at the SMD/B3LYP-D3/6–31G(d) level of theory. Dashed line: NPO (**5**); solid line: NMO (**4**). ΔG in kcal mol^{-1}.

than **TS1** (see the Supplementary Material). Examining the corresponding calculations for NMO (**4**) (Fig. 1, solid line), the energy profile for azomethine ylid formation is very similar to that for NPO (**5**). Indeed, the overall free energy barrier (**22** → **TS2**) for NMO (**4**) is 2.2 kcal mol^{-1} smaller than that for NPO (**5**). Thus, azomethine ylid formation from NMO (**4**) via a Roussi-type mechanism appears to be more facile than the corresponding reaction of NPO (**5**), and the low yields of cycloadduct obtained using NMO (**4**) cannot be ascribed to any inherent lack of reactivity of NMO towards ylid formation.

The calculations reveal that a crucial factor differentiating the chemistry of NMO (**4**) from that of NPO (**5**) and other aliphatic *N*-oxides is the regioselectivity of the initial deprotonation step. The availability of alternative deprotonation routes for NMO leads to a complex set of reaction pathways as depicted in Fig. 2. Whereas for NPO (**5**) deprotonation at *N*Me (*exo* deprotonation) is kinetically favoured by 1.5 kcal mol^{-1}, the preferred site of deprotonation of NMO (**4**) is not *N*-Me but *N*-CH_2, leading to the endocyclic carbanion **23**. The *endo* deprotonation TS (**TS4**) for NMO with $LiNMe_2$ lies 2 kcal mol^{-1} lower in energy than the *exo* TS (**TS1**). Similar *endo* selectivities of ~2 kcal mol^{-1} are computed for the K^+ and Mg^{2+} bases. The switch in the regioselectivity of deprotonation on going from NPO (**5**) to NMO (**4**) is stereoelectronic in origin. In NMO, the equatorial *N*-CH_2 proton is antiperiplanar to the C–O bond, allowing the *endo* deprotonation TS (and the resulting carbanion) to be stabilised by negative hyperconjugation (see $\mathbf{TS4_{Li}}$, Fig. 2).

Each of the observed products **6**, **7**, **14**, and **15** can be accessed via multiple mechanistic pathways. In principle, cycloadduct **6** could be formed by the sequence of *N*-oxide deprotonation, N–O cleavage, and iminium ion deprotonation following either an *exo* or *endo* mode (Path A or Path B1, respectively, in Fig. 2) followed by 1,3-dipolar cycloaddition. Pyrrole **7** may (as proposed above) be derived from cycloadduct **6** by the action of base (Path A or Path B1), or it may alternatively arise via Path B2, which consists of nucleophilic addition by the *endo* carbanion **23** to diphenyl acetylene (i.e. **24**), followed by intramolecular proton transfer (i.e. **25**), N–O cleavage (i.e. **26**), deprotonation and 6π-electrocyclic ring closure[26] of the resulting ylid **27** to intermediate **28**,[27] followed by base-catalysed tautomerisation. The acyclic hydroxylamine **14** and five-membered *N*-oxide **15** are interconvertible by (reverse) Cope elimination, an intramolecular process. The equilibrium positions of Cope eliminations are known to depend on solvent, chloroform favouring cyclisation.[19f] *N*-Oxide **15** could be formed from the *endo* carbanion **23** through a sequence consisting of C–O bond cleavage to **29** followed by 5-*exo*-*trig* cyclisation (Path B3). Alternatively, deprotonation of NMO (**4**) α to the endocyclic oxygen atom (Path C) would give carbanion **30**, which may undergo C–N bond cleavage to give **14**. The energies of the important intermediates and transition states along these pathways coordinated to different metal cations are shown in Fig. 2. Energies are reported only for the transition states and intermediates preceding the loss of metal oxide. Because the loss of metal oxide provides a very large thermodynamic driving force, the subsequent steps are not rate-limiting. Details of the barriers of the downstream steps are included in the Supplementary Material.

The energies of the transition states along Paths A and B1 (via **19** or **27**, respectively) provide insights into the propensities of different bases to yield cycloadduct **6**. Starting from either the *exo* carbanion **21** or the kinetically favoured *endo* carbanion **23**, the rate-determining N–O cleavage steps (**TS2** and **TS5**) are low in energy when the metal cation is Mg^{2+} ($\Delta G^{\ddagger} \approx -2$ kcal mol^{-1}), high in energy for K^+ (≥21 kcal mol^{-1}), and intermediate for Li^+ (6–8 kcal mol^{-1}). The Mg^{2+} cation promotes N–O cleavage because it is a small cation with a high charge density, which allows strong binding to the O^{2-} that is being abstracted from the carbanion. Conversely, the large monocation K^+ provides the weakest stabilisation of the oxide. These results are in agreement with the propensity towards cycloadduct formation observed experimentally with different metal cations, where an isolable quantity of **6** was obtained using MDA, no **6** was obtained using KH or KHMDS, and the use of LDA gave pyrrole **7**, a decomposition product of **6**. Pyrrole **7** is computed to be 21 kcal mol^{-1} lower in energy than cycloadduct **6**, and hence the equilibrium position of the base-catalysed interconversion of

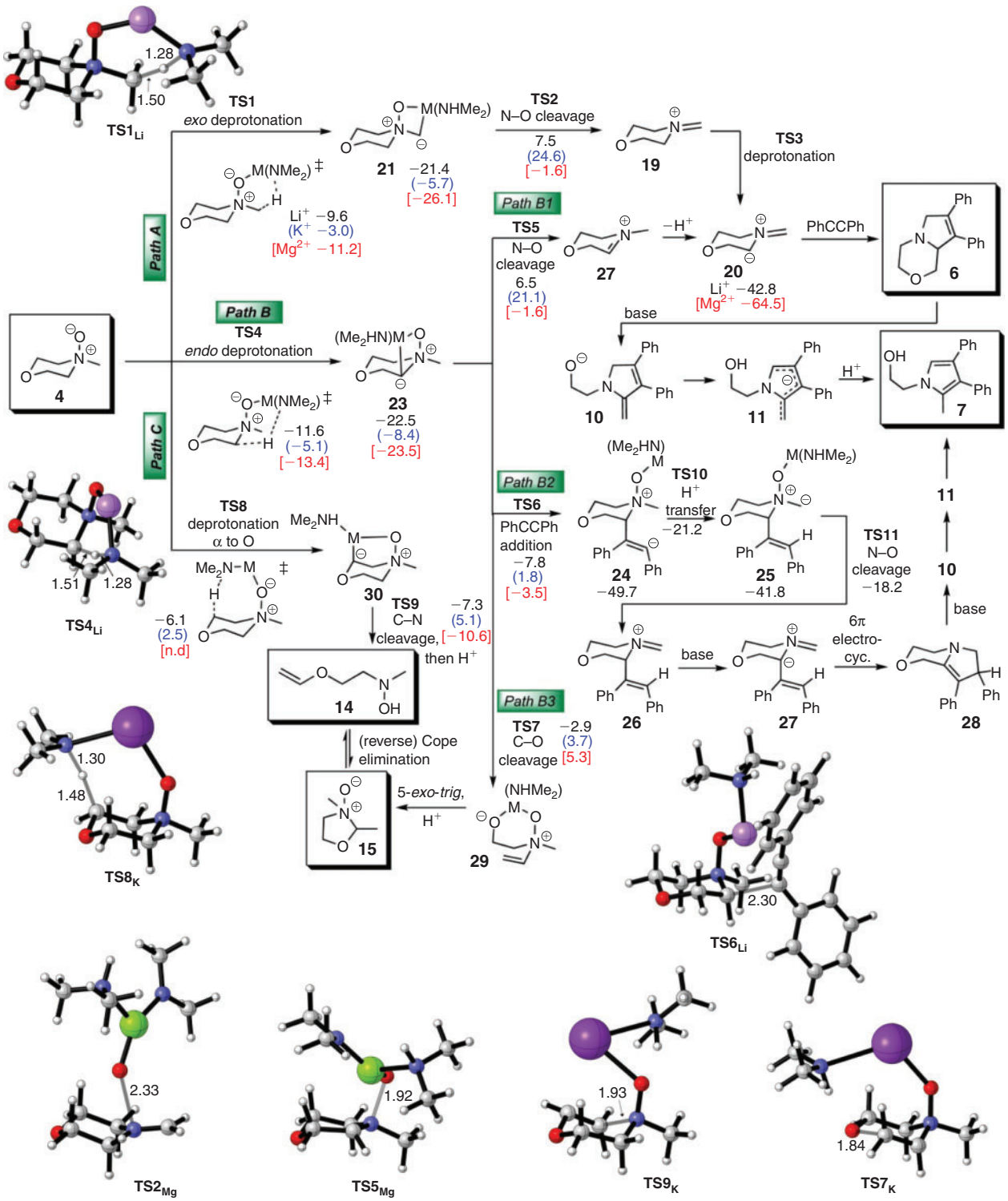

Fig. 2. Pathways for deprotonation of NMO (**4**) and conversion of the three regioisomeric carbanions (**21**, **23**, and **30**) to the observed products (**6**, **7**, **14**, and **15**). Free energies (kcal mol^{-1}) of selected species complexed to different metal cations are shown. Li^+ numbers shown in normal type; K^+ numbers shown in parentheses; Mg^{2+} numbers shown in square brackets.

6 and **7** lies strongly in favour of **7**. That **6** is decomposed by excess LDA, but not by excess MDA, may reflect differences in steric effects that may hamper the deprotonation of **6** to give **10** when the base is MDA.

Alternatively, pyrrole **7** can be accessed through Path B2. It is noteworthy that the initial step of this pathway (addition of *endo* carbanion **23** to diphenyl acetylene giving **24**) is most facile for Li^+ (**TS6**). Indeed, for Li^+, nucleophilic addition to the alkyne via **TS6** is favoured by 14.3 kcal mol^{-1} over N–O cleavage via **TS5**. With Mg^{2+}, nucleophilic addition to the alkyne via **TS6** is favoured also, but only by 2 kcal mol^{-1}. Given the simple model species used, and the fact that the rate of passage through **TS6** (but not **TS5**) is dependent on alkyne concentration, it is unlikely that such a small difference in barriers would be a reliable

predictor of differences in reaction rates. The main conclusions that can be drawn from the calculated data are that Li^+ promotes reaction through Path B2, and Mg^{2+} provides strong stabilisation to the N–O cleavage transition states involved in ylid formation via Paths A and B1.

Concerning products **14** and **15**, which have not incorporated any alkyne and are obtained only with potassium bases, the calculations indicate that when $M^+ = K^+$, the preferred reaction of the thermodynamic *endo* carbanion **23** is Path B2. However, Path B3 leading to **14** and **15** via **TS7** lies only 2 kcal mol^{-1} higher in energy, again within the error expected from these simple models. Transition state **TS7** (C–O cleavage) is also predicted to be relatively low in energy when the metal ion is Li^+ (−2.9 kcal mol^{-1}), but no formation of **14** or **15** is observed using Li^+ bases since Path B2 leading to pyrrole **7** is preferred.

In the alternative mechanism leading to **14** and/or **15** (Path C), the initial TS (**TS8**, deprotonation α to oxygen) has $\Delta G^{\ddagger} = 2.5$ kcal mol^{-1} for $M^+ = K^+$, which is ≥5 kcal mol^{-1} higher than the TSs for *exo* or *endo* deprotonation of NMO (**TS1**, **TS4**). If the deprotonation of NMO is kinetically controlled, then the calculations predict that the route to **14** and/or **15** is Path B3. However, the overall rate-determining transition state in Path C (**TS9**, C–N cleavage in carbanion **30**) with $M^+ = K^+$ lies at 5.1 kcal mol^{-1}, only 1.4 kcal mol^{-1} higher than the rate-determining TS in Path B3 (**TS7**, C–O cleavage in carbanion **23**). Taking into account the approximations inherent in the calculations (see above), the small difference between these barriers suggests that under conditions of thermodynamic control, both Path B3 and Path C are feasible for K^+ bases.

The possibility that the reactions of NMO (**4**) with bases may follow radical mechanisms was explored by conducting a reaction in the presence of (2,2,6,6-tetramethylpiperidin-1-yl) oxidanyl (TEMPO), in an attempt to trap any radical intermediates. No TEMPO adducts were detected when the reaction of NMO (**4**) with diphenyl acetylene was run in the presence of TEMPO, and the reaction outcome remained unaltered from that obtained in the absence of TEMPO.[28]

Lastly, we considered the possibility that the differences in observed products obtained from NMO (**4**) and NPO (**5**) may result from differences in the reactive conformation of the *N*-oxide. It is well known that cyclic *N*-oxides can exist as an equilibrium mixture of conformers, and in the case of NPO (**5**) the *O*-axial conformer has been determined to be the major conformer (95 %).[29c] The ^{1}H NMR spectrum of NMO (**4**) showed only a single set of signals (at 25°C), confirming the results reported by Pohl et al. that the axial is the major conformer.[29c] Calculations indicate that the *O*-axial conformer of NMO (**4**) is favoured by 2.8 kcal mol^{-1}, which is 0.7 kcal mol^{-1} greater than the *O*-axial preference of NPO (**5**) (2.1 kcal mol^{-1}) (see also Pohl et al.[29c]). Additionally, the *O*-axial conformers of both *N*-oxides are computed to undergo deprotonation more readily than the *O*-equatorial conformers. These results suggest that Roussi reactions involving NMO (**4**) and NPO (**5**) both involve the *O*-axial conformers.

Conclusion

The Roussi reaction is one of only a handful of procedures that allow NAYs to be generated at low temperature. The study reported herein describes a detailed investigation into the complex array of reactions undergone by NMO (**4**) under Roussi's conditions. We have found that the base counterion (i.e. metal cation) has a critical role in directing the course of reaction and that Li^+, Na^+, K^+, and Mg^{2+} cations each produce a different outcome – a highly unusual result. Based on our studies, MDA has emerged as the base of choice for the formation of **6**, avoiding an otherwise elimination–aromatisation sequence affording pyrrole **7** under LDA conditions. This finding is likely to hold true in other morpholine containing heterocycles generated under these conditions.

General Experimental

^{1}H and ^{13}C NMR spectra were recorded on Bruker AV300 (300.13, 75.47 MHz) and DRX500 (500.13, 125.76 MHz) instruments in $CDCl_3$ unless otherwise stated. Coupling constants are given in Hz and chemical shifts are expressed as δ values in ppm. High resolution electrospray ionisation (HRESIMS) accurate mass measurements were recorded in positive mode on a Bruker MicrOTOF-Q (quadrupole–time of flight) instrument with a Bruker ESI source using sodium formate as a reference calibrant. Column chromatography was undertaken on silica gel (flash silica gel, 230–400 mesh) with distilled solvents. All reagents and solvents were purified before use according to literature methods.[30] NMO (**4**) was dried at 45°C, 0.1 mmHg, for a period of 2 h before use. THF was freshly distilled from a sodium/benzophenone still. Fine chemicals were purchased from Sigma-Aldrich.

Computational Methods

DFT calculations were performed using the *Gaussian 09* software.[31] Geometries were optimised at the B3LYP/6–31G(d) level of theory in the gas phase.[32] Stationary points were characterised by vibrational frequency calculations at this level, and transition states were further verified by means of IRC calculations.[33] Single-point calculations at the B3LYP/6–31G(d) level using the SMD implicit solvent model were performed to obtain solvation energies in THF.[34] Dispersion energy corrections were computed for the gas-phase geometries using Grimme's D3 model[35] with Becke–Johnson damping.[36] Free energies in THF solution (25°C) were obtained by adding the SMD solvation energy and D3 dispersion energy to the B3LYP/6–31G(d) gas-phase free energy and were corrected to a standard state of 1 mol L^{-1}.

Experimental

1-N-(2-Hydroxyethyl)-2-methyl-3, 4-diphenyl-1H-pyrrole (7)

A mixture of NMO (**4**) (235 mg, 2.01 mmol) and diphenyl acetylene (357 mg, 2.01 mmol) in anhydrous THF (10 mL) under an argon atmosphere was treated with freshly prepared LDA (12.5 mL, 0.56 M in THF) at 0°C. The reaction was stirred at this temperature for a period of 4 h and a further 17 h at r.t. after which time the reaction was quenched by the addition of a minimal amount of $NH_4Cl_{(aq)}$. The solvent was removed under vacuum using a liquid nitrogen trap to afford a crude mixture. Purification by silica column chromatography (light petroleum : EtOAc, 2 : 1) afforded **7** (16.3 mg, 34 %) as a pale yellow oil. δ_H (500 MHz, $CDCl_3$) 7.33–7.28 (m, 2H), 7.25–7.09 (m, 8H), 6.84 (s, 1H), 4.07 (t, *J* 5.5, 2H), 3.94 (t, *J* 5.5, 2 H), 2.26 (s, 3 H). δ_C (125 MHz, $CDCl_3$) 136.3, 135.7, 130.5, 128.0 (2C), 127.9, 126.9, 125.6, 125.2, 123.4, 120.8, 118.5, 62.5, 49.1, 10.5. HRMS Anal. Calc. for $C_{19}H_{20}NO$: 278.1539; found: 278.1541.

2-(N-Ethyl-N-methylamino)ethan-1-ol (13)

To neat *N*-methyl-ethanolamine (0.86 mL, 10.65 mmol) at 0°C was added ethylbromide (0.80 mL, 10.65 mmol) dropwise. After 20 min at 0°C the ice bath was removed. Upon warming an

exotherm was observed. When no further heat was generated (30 min) the reaction was cooled to 0°C and a further portion of ethylbromide (0.20 mL, 0.25 equiv.) was added and the ice bath was removed. After stirring at r.t. for a period of a 100 min gentle vacuum was applied to remove volatiles and the crude was washed with acetone. After applying gentle vacuum to remove the remaining acetone, excess solid pellets of NaOH was added and the mixture was stirred for a period of 30 min. The crude residue was placed under high vacuum (~0.1 Torr) and the product was captured using a liquid nitrogen trap. When most of the product was captured, the crude was slowly heated to 60°C for a brief period to afford the tertiary amine **13** (527 mg, 48 %) as a colourless liquid. δ_H (300 MHz, $CDCl_3$) 3.58 (dd, *J* 5.5, 2H), 2.55–2.44 (m, 4H), 2.24 (s, 3H), 1.06 (t, *J* 7.1, 3H). This material is commercially available.

N-*Ethyl*-2-*hydroxy*-N-*methylethan*-1-*amine* N-*oxide* (***12***)

To neat compound **13** (322 mg, 3.12 mmol) was added H_2O_2 (0.41 μL, 30 % aqueous solution) and the resulting mixture was stirred overnight (20 h). Toluene was then added with vigorous stirring, and after ~5 min the solvent was removed under high vacuum to afford the title compound **12** (314 mg, 84 %) as a viscous clear oil. δ_H (500 MHz, [D4]methanol) 4.07–3.96 (m, 2H), 3.52–3.39 (m, 4H), 3.18 (s, 3H), 1.36 (t, *J* 7.2, 3H). δ_C (125 MHz, [D4]methanol) 70.1, 65.7, 57.2, 55.3, 8.8. HRMS Anal. Calc. for $C_5H_{14}NO_2$: 120.1019; found: 120.1019.

N-*Methyl*-N-*(2-(vinyloxy)ethyl)hydroxylamine* (***14***) *and 2,3-dimethyloxazolidine 3*-N-*oxide* (***15***)

A suspension of NMO (**4**) (137 mg, 1.17 mmol) and diphenyl acetylene (208 mg, 1.17 mmol) in anhydrous THF (10 mL) was treated with KHMDS (9.36 mL, 0.5 M in toluene) at 0°C under an argon atmosphere. The reaction was stirred at this temperature for a period of 1 h and a further 24 h at r.t. after which time the reaction was quenched using a saturated aqueous solution of NH_4Cl. The aqueous phase was extracted using EtOAc, dried over $MgSO_4$, and concentrated under vacuum to afford hydroxylamine **14** as a crude oil. δ_H (500 MHz, [D6]benzene) 6.47 (dd, *J* 14.3, 6.6, 1H, **14**), 4.25 (dd, *J* 14.3, 1.8, 1H, **14**), 4.18–4.12 (m, 1H, **15**), 3.97 (dd, *J* 6.6, 1.8, 1H, **14**), 3.83 (br s, 2H, **14**), 3.71 (q, *J* 5.5, 1H, **15**), 3.43 (ddd, *J* 10.5, 7.2, 3.3, 1H, **15**), 3.23 (dt, *J* 8.1, 3.3, 1H, **15**), 2.76 (br t, *J* 5.5, 2H, **14**), 2.53 (br s, 3H, **14**), 2.45 (s, 3H, **15**), 2.46–2.39 (m, 1H, **15**), 1.32 (d, *J* 5.5, 3H, **15**). δ_C (125 MHz, [D6]benzene) 152.6 (**14**), 100.1 (**15**), 86.4 (**14**), 67.0 (**15**), 66.5 (**14**), 64.2 (**15**), 61.6 (**14**), 52.6 (**14**), 49.7 (**15**), 13.0 (**15**). Compound **14** converts to **15** in chloroform-d and [D6]benzene; thus, only a mixture could be observed by NMR.

The crude oil was dissolved in $CHCl_3$ (used as obtained from supplier) and stirred for a period of 20 h at r.t. after which time the solvent was removed under vacuum and the crude material washed with light petroleum to afford oxazolidine *N*-oxide **15** (110 mg, 80 %) as a pale solid. δ_H (500 MHz, $CDCl_3$) 4.64 (q, *J* 5.5, 1H), 4.46 (dt, *J* 8.6, 7.3, 1H), 4.06 (dt, *J* 8.6, 4.0, 1H), 3.79 (ddd, *J* 10.9, 7.2, 3.9, 1H), 3.71–3.63 (m, 1H), 3.20 (s, 3H), 1.54 (d, *J* 5.5, 3H). δ_C (125 MHz, $CDCl_3$) 100.4, 67.6, 63.9, 53.3, 12.6. HRMS Anal. Calc. for $C_5H_{12}NO_2$: 118.0863; found: 118.0858.

*7,8-Diphenyl-3,4,6,8a-tetrahydro-1*H-*pyrrolo[2,1-c][1,4]oxazine* (***6***)

To a suspension of NMO (**4**) (252 mg, 2.15 mmol) and diphenyl acetylene (383 mg, 2.15 mmol) in anhydrous THF (14 mL) at 0°C under an argon atmosphere, was added MDA (9.22 mL, 6.45 mmol, 0.7 M THF solution) dropwise over a period of 10 min (effervescence was observed over the course of few min and the reaction became homogeneous and yellow in colour). The reaction was allowed to slowly reach r.t. and was subsequently quenched (saturated aqueous solution of NH_4Cl) 3 h after addition of MDA. The aqueous phase was extracted using EtOAc, and the combined organic phase was washed with brine and dried over $MgSO_4$. The crude mixture was purified by silica column chromatography (EtOAc) to afford **6** (109 mg, 18 %) as a colourless oil. δ_H (500 MHz, $CDCl_3$) 7.31–7.14 (m, 10H), 4.29 (dd, *J* 12.8, 3.7, 1H), 4.11 (dq, *J* 9.6, 3.6, 1H), 3.88 (dd, *J* 12.7, 3.4, 1H), 3.85 (dd, *J* 11.0, 3.6, 1H), 3.78–3.72 (m, 2H), 3.52 (dd, *J* 11.2, 9.6, 1H), 3.08 (ddd, *J* 12.7, 8.7, 5.7, 1H), 2.97 (dt, *J* 12.7, 2.7, 1H). δ_C (125 MHz, $CDCl_3$) 136.9, 136.1, 135.0, 134.9, 128.6, 128.3, 128.2, 127.8, 127.4, 127.3, 68.3, 68.1, 64.3, 60.4, 48.6. HRMS Anal. Calc. for $C_{19}H_{20}NO$: 278.1539; found: 278.1532.

1-N-*(2-Hydroxyethyl)-2-methyl-3,4-diphenyl-1*H-*pyrrole* (***7***) *from LDA Treatment of* ***6***

To a solution of **6** (90 mg, 0.324 mmol) in anhydrous THF (9 mL) at 0°C under an argon atmosphere, was added freshly prepared LDA (3.0 mL, 1.14 mmol, 0.37 M THF solution) in three portions at 30 min intervals. The reaction was quenched 15 min after the last addition using a saturated aqueous solution of NH_4Cl. The aqueous phase was extracted using EtOAc, and the combined organic phase was dried over $MgSO_4$. Purification by silica column chromatography (EtOAc) afforded **7** (64 mg, 71 %, 82 % brsm) and recovered starting material **6** (12 mg).

Dimorpholinomethane (***16***)

To a suspension of NMO (**4**) (412 mg, 3.51 mmol) in anhydrous THF (20 mL) under an argon atmosphere, was added MDA (7.54 mL, 5.27 mmol, 0.7 M THF solution) dropwise over a period of 15 min. The reaction was quenched 1 h after the addition using a saturated aqueous solution of NH_4Cl. The aqueous phase was extracted using EtOAc and the combined organic phase was dried over $MgSO_4$ to afford **16** in a crude yield of ~70 %. The NMR spectra were in accordance with those reported previously.[24]

Supplementary Material

Copies of ^1H and ^{13}C NMR spectra, further discussion of computational studies of mechanism, and a compilation of computational data can be found in the Supplementary Material.

Acknowledgements

We thank the Australian Research Council and the University of Queensland for financial support. C.M.W. and E.H.K. are ARC Future Fellows supported by grants FT110100851 and FT120100632, respectively. Computational resources were provided by the National Facility of the National Computational Infrastructure through the Merit Allocation Scheme, and by the University of Queensland Research Computing Centre.

References

[1] (a) I. Coldham, R. Hufton, *Chem. Rev.* **2005**, *105*, 2765. doi:10.1021/CR040004C
(b) W. H. Pearson, P. Stoy, *Synlett* **2003**, 903. doi:10.1055/S-2003-39285
(c) E. Vedejs, F. G. West, *Chem. Rev.* **1986**, *86*, 941. doi:10.1021/CR00075A014
(d) K. V. Gothelf, K. A. Jorgensen, *Chem. Rev.* **1998**, *98*, 863. doi:10.1021/CR970324E
(e) C. Najera, J. M. Sansano, *Curr. Org. Chem.* **2003**, *7*, 1105. doi:10.2174/1385272033486594

(f) L. M. Harwood, R. J. Vickers, in *Synthetic Applications of 1,3-Dipolar Cycloaddition Chemistry Toward Heterocycles and Natural Products* (Eds. A. Padwa, W. H. Pearson) **2003**, Vol. 59, Ch. 3, pp. 169–252.

[2] (a) See for example: I. Coldham, S. Jana, L. Watson, N. G. Martin, *Org. Biomol. Chem.* **2009**, *7*, 1674. doi:10.1039/B822743H
(b) N. Shimada, Y. Abe, S. Yokoshima, T. Fukuyama, *Angew. Chem. Int. Ed.* **2012**, *51*, 11824. doi:10.1002/ANIE.201206863
(c) A. J. M. Burrell, I. Coldham, L. Watson, N. Oram, C. D. Pilgram, N. G. Martin, *J. Org. Chem.* **2009**, *74*, 2290. doi:10.1021/JO8019913
(d) A. J. M. Burrell, I. Coldham, N. Oram, *Org. Lett.* **2009**, *11*, 1515. doi:10.1021/OL9001653
(e) A. J. M. Burrell, I. Coldham, *Curr Org Synth* **2010**, *7*, 312. doi:10.2174/157017910791414472
(f) C. Fang, C. S. Shanahan, D. H. Paull, S. F. Martin, *Angew. Chem. Int. Ed.* **2012**, *51*, 10596. doi:10.1002/ANIE.201205274

[3] (a) See for example: C. Ménard-Moyon, N. Izard, E. Doris, C. Mioskowski, *J. Am. Chem. Soc.* **2006**, *128*, 6552. doi:10.1021/JA060802F
(b) V. Georgakilas, K. Kordatos, M. Prato, D. M. Guldi, M. Holzinger, A. Hirsch, *J. Am. Chem. Soc.* **2002**, *124*, 760. doi:10.1021/JA016954M

[4] See for example: S. Pandiancherri, D. W. Lupton, *Tetrahedron Lett.* **2011**, *52*, 671 and references therein. doi:10.1016/J.TETLET.2010.11.142

[5] See for example: R. J. Carra, M. T. Epperson, D. Y. Gin, *Tetrahedron* **2008**, *64*, 3629. doi:10.1016/J.TET.2008.02.008

[6] (a) See for example: P. Deprez, J. Royer, H.-P. Husson, *Tetrahedron: Asymmetry* **1991**, *2*, 1189. doi:10.1016/S0957-4166(00)80019-1
(b) P. Deprez, J. Rouden, A. Chiaroni, C. Riche, J. Royer, H.-P. Husson, *Tetrahedron Lett.* **1991**, *32*, 7531. doi:10.1016/0040-4039(91)80526-C

[7] (a) R. Beugelmans, G. Negron, G. Roussi, *J. Chem. Soc., Chem. Commun.* **1983**, 31. doi:10.1039/C39830000031
(b) G. Roussi, *Trends Org. Chem.* **1993**, *4*, 101.

[8] (a) For additional examples, see: S. Takano, Y. Sugihara, K. Ogasawara, *Heterocycles* **1992**, *34*, 1519. doi:10.3987/COM-92-6107
(b) J. E. Davoren, D. L. Gray, A. R. Harris, D. M. Nason, W. Xu, *Synlett* **2010**, 2490. doi:10.1055/S-0030-1258026
(c) B. De, J. F. DeBernardis, R. Prasad, *Synth. Commun.* **1988**, *18*, 481. doi:10.1080/00397918808060740
(d) G. Negrón, A. Fuentes, M. Romero, G. Madrid, R. Cruz, *Rev. Soc. Quím. Méx.* **1999**, *43*, 123.

[9] (a) D. Bernier, U. K. Efelscheid, S. Woodward, *Org. Prep. Proced. Int.* **2009**, *41*, 173. doi:10.1080/00304940902955756
(b) A. Albini, *Synthesis* **1993**, 263. doi:10.1055/S-1993-25843

[10] G. Roussi, *Heterocycles* **1990**, *31*, 1445. doi:10.3987/COM-90-5321

[11] R. Beugelmans, L. Bemadjilal-Iguestira, J. Chastanet, G. Negron, G. Roussi, *Can. J. Chem.* **1985**, *63*, 725. doi:10.1139/V85-120

[12] J. Chastanet, G. Roussi, *J. Org. Chem.* **1988**, *53*, 3808. doi:10.1021/JO00251A026

[13] G. Negron, G. Roussi, J. Zhang, *Heterocycles* **1992**, *34*, 293. doi:10.3987/COM-91-5900

[14] G. Roussi, J. Zhang, *Tetrahedron* **1991**, *47*, 5161. doi:10.1016/S0040-4020(01)87128-3

[15] (a) J. Chastanet, H. Fathallah, G. Negron, G. Roussi, *Heterocycles* **1992**, *34*, 1565. doi:10.3987/COM-92-6052
(b) J. Chastanet, G. Roussi, G. Negrón, *Carbohydr. Res.* **1995**, *268*, 301. doi:10.1016/0008-6215(94)00331-9

[16] G. Roussi, J. Zhang, *Tetrahedron Lett.* **1991**, *32*, 1443. doi:10.1016/0040-4039(91)80353-8

[17] (a) J. Chastanet, G. Roussi, *J. Org. Chem.* **1985**, *50*, 2910. doi:10.1021/JO00216A020
(b) J. Chastanet, G. Roussi, *Heterocycles* **1985**, *23*, 653. doi:10.3987/R-1985-03-0653

[18] M. Schlosser, *Pure Appl. Chem.* **1988**, *60*, 1627. doi:10.1351/PAC198860111627

[19] (a) A. C. Cope, N. A. Lebel, *J. Am. Chem. Soc.* **1960**, *82*, 4656. doi:10.1021/JA01502A052
(b) C. H. DePuy, R. W. King, *Chem. Rev.* **1960**, *60*, 431. doi:10.1021/CR60207A001
(c) H. O. House, D. T. Manning, D. G. Melillo, L. F. Lee, O. R. Haynes, B. E. Wilkes, *J. Org. Chem.* **1976**, *41*, 855. doi:10.1021/JO00867A023
(d) D. St. C. Black, J. E. Doyle, *Aust. J. Chem.* **1978**, *31*, 2317. doi:10.1071/CH9782317
(e) E. Ciganek, *J. Org. Chem.* **1990**, *55*, 3007. doi:10.1021/JO00297A011
(f) E. Ciganek, J. M. Read, Jr, J. C. Calabrese, *J. Org. Chem.* **1995**, *60*, 5795. doi:10.1021/JO00123A013
(g) W. Oppolzer, A. C. Spivey, C. G. Bochet, *J. Am. Chem. Soc.* **1994**, *116*, 3139. doi:10.1021/JA00086A060
(h) N. J. Cooper, D. W. Knight, *Tetrahedron* **2004**, *60*, 243. doi:10.1016/J.TET.2003.10.043
(i) E. H. Krenske, E. C. Davison, I. T. Forbes, J. A. Warner, A. L. Smith, A. B. Holmes, K. N. Houk, *J. Am. Chem. Soc.* **2012**, *134*, 2434. doi:10.1021/JA211568K

[20] (a) For this work, sodium *N*,*N*-diisopropylamide (NDA) was generated in situ from *n*-butyl lithium, *N*,*N*-diisopropylamine and sodium *t*-butoxide in THF using a similar procedure to that described by L. Lochmann, J. Trekoval, *J. Organomet. Chem.* **1979**, *179*, 123. doi:10.1016/S0022-328X(00)95213-6
(b) For isolation of NDA see: T. Munguia, Z. A. Bakir, F. Cervantes-Lee, A. Metta-Magana, K. H. Pannell, *Organometallics* **2009**, *28*, 5777. doi:10.1021/OM9006032

[21] P. E. Eaton, C.-H. Lee, Y. Xiong, *J. Am. Chem. Soc.* **1989**, *111*, 8016. doi:10.1021/JA00202A054

[22] (a) D. B. Collum, *Acc. Chem. Res.* **1992**, *25*, 448. doi:10.1021/AR00022A003
(b) R. E. Mulvey, S. D. Robertson, *Angew. Chem. Int. Ed.* **2013**, *52*, 11470. doi:10.1002/ANIE.201301837

[23] D. Grierson, *Org. React.* **1990**, *39*, 85.

[24] A. Porzelle, C. M. Williams, *Synthesis* **2006**, 3025.

[25] (a) T. Rosenau, A. Potthast, P. Kosma, C.-L. Chen, J. S. Gratzl, *J. Org. Chem.* **1999**, *64*, 2166. doi:10.1021/JO982350Y
(b) T. Rosenau, A. Potthast, P. Kosma, *Tetrahedron* **2002**, *58*, 9809. doi:10.1016/S0040-4020(02)01291-7
(c) For further studies on the degradation of NMO, see: T. Rosenau, A. Potthast, P. Kosma, *Tetrahedron* **2004**, *60*, 301. doi:10.1016/J.TET.2003.11.015
(d) F. Liebner, P. Schmid, C. Adelwöhrer, T. Rosenau, *Tetrahedron* **2007**, *63*, 11817. doi:10.1016/J.TET.2007.09.055
(e) Furthermore, see: T. Rosenau, A. Potthast, H. Sixta, P. Kosma, *Prog. Polym. Sci.* **2001**, *26*, 1763. doi:10.1016/S0079-6700(01)00023-5

[26] (a) E. Taylor, I. J. Turchi, *Chem. Rev.* **1979**, *79*, 181. doi:10.1021/CR60318A003
(b) R. Huisgen, *Angew. Chem. Int. Ed. Engl.* **1980**, *19*, 947 [*Angew. Chem.* **1980**, *92*, 979]. doi:10.1002/ANIE.198009473
(c) T. M. V. D. Pinho e Melo, *Eur. J. Org. Chem.* **2006**, 2873. doi:10.1002/EJOC.200500892

[27] An alternative pathway, calculated to be low in energy, involves ring closure by intramolecular alkylation of iminium cation **26**.

[28] Using the radical trapping agent γ-tocopherol, Kosma and co-workers identified the radical intermediates derived from reduction of NMO (**4**) with Fe^{II}, Mn^{II}, or Co^{II} salts. Radical pathways were shown to lead to decomposition of NMO (**4**) to *N*-methyl morpholine, morpholine, and formaldehyde. See: T. Rosenau, A. Potthast, H. Sixta, P. Kosma, *Tetrahedron* **2002**, *58*, 3073. doi:10.1016/S0040-4020(02)00163-1

[29] (a) A. Katritzky, *J. Chem. Soc. B* **1971**, 1330.
(b) Y. Shvo, E. D. Kaufman, *J. Org. Chem.* **1981**, *46*, 2148 and references therein. doi:10.1021/JO00323A035
(c) R. Pohl, M. Dračínský, L. Slavětínská, M. Buděšínský, *Magn. Reson. Chem.* **2011**, *49*, 320. doi:10.1002/MRC.2750

[30] D. D. Perrin, W. L. F. Armarego, *Purification of Laboratory Chemicals,* 3rd edn **1988** (Pergamon Press: Oxford).

[31] M. J. Frisch, G. W. Trucks, H. B. Schlegel, G. E. Scuseria, M. A. Robb, J. R. Cheeseman, G. Scalmani, V. Barone, B. Mennucci,

G. A. Petersson, H. Nakatsuji, M. Caricato, X. Li, H. P. Hratchian, A. F. Izmaylov, J. Bloino, G. Zheng, J. L. Sonnenberg, M. Hada, M. Ehara, K. Toyota, R. Fukuda, J. Hasegawa, M. Ishida, T. Nakajima, Y. Honda, O. Kitao, H. Nakai, T. Vreven, J. A. Montgomery, Jr, J. E. Peralta, F. Ogliaro, M. Bearpark, J. J. Heyd, E. Brothers, K. N. Kudin, V. N. Staroverov, R. Kobayashi, J. Normand, K. Raghavachari, A. Rendell, J. C. Burant, S. S. Iyengar, J. Tomasi, M. Cossi, N. Rega, J. M. Millam, M. Klene, J. E. Knox, J. B. Cross, V. Bakken, C. Adamo, J. Jaramillo, R. Gomperts, R. E. Stratmann, O. Yazyev, A. J. Austin, R. Cammi, C. Pomelli, J. W. Ochterski, R. L. Martin, K. Morokuma, V. G. Zakrzewski, G. A. Voth, P. Salvador, J. J. Dannenberg, S. Dapprich, A. D. Daniels, O. Farkas, J. B. Foresman, J. V. Ortiz, J. Cioslowski, D. J. Fox, *Gaussian 09, Revision A.02* **2009** (Gaussian, Inc.: Wallingford, CT).

[32] (a) C. Lee, W. Yang, R. G. Parr, *Phys. Rev. B* **1988**, *37*, 785. doi:10.1103/PHYSREVB.37.785
(b) A. D. Becke, *J. Chem. Phys.* **1993**, *98*, 1372. doi:10.1063/1.464304
(c) A. D. Becke, *J. Chem. Phys.* **1993**, *98*, 5648. doi:10.1063/1.464913
(d) P. J. Stephens, F. J. Devlin, C. F. Chabalowski, M. J. Frisch, *J. Phys. Chem.* **1994**, *98*, 11623. doi:10.1021/J100096A001

[33] (a) C. Gonzalez, H. B. Schlegel, *J. Chem. Phys.* **1989**, *90*, 2154. doi:10.1063/1.456010
(b) C. Gonzalez, H. B. Schlegel, *J. Phys. Chem.* **1990**, *94*, 5523. doi:10.1021/J100377A021

[34] A. V. Marenich, C. J. Cramer, D. G. Truhlar, *J. Phys. Chem. B* **2009**, *113*, 6378. doi:10.1021/JP810292N

[35] S. Grimme, J. Antony, S. Ehrlich, H. Krieg, *J. Chem. Phys.* **2010**, *132*, 154104. doi:10.1063/1.3382344

[36] S. Grimme, S. Ehrlich, L. Goerigk, *J. Comput. Chem.* **2011**, *32*, 1456. doi:10.1002/JCC.21759